Nonlinear Temperature Control of a Batch Suspension Polymerization Reactor

MOHAMMAD SHAHROKHI* *and* MOHAMMAD ALI FANAEI

Dept. of Chemical Engineering
Sharif University of Technology
Tehran, Iran

This paper concerns nonlinear temperature control of a batch polymerization reactor where suspension polymerization of methyl methacrylate (MMA) takes place. For this purpose, four control algorithms, namely, a fix proportional-integral (PI) controller, an adaptive proportional-integral-derivative (PID) controller and two globally linearizing control (GLC) schemes, one for known kinetic model (GLC-I) and the other for unknown kinetic model (GLC-II), are selected. The performances of these controllers are compared through simulation and real-time studies in the presence of different levels of parameter uncertainty. The results indicate that GLC-I and GLC-II have better performances than fix PI and adaptive PID, especially in case of strong gel effect. The worst performance belongs to adaptive PID because of rapid model changes in gel effect region. GLC-II has a simpler structure than GLC-I and can be used without requiring the kinetic model. In implementation of GLC-I the closed loop observer should be used because of model uncertainties.

INTRODUCTION

In the polymerization industry there is considerable economic incentive to produce polymers with desired end-use properties. The development of operating policies that will result in the production of polymers with desired end-use properties is called "quality control." Reaction temperature is the most important operating variable in the quality control of polymerization reactors. Minimization of temperature excursions from the setpoint (in both isothermal or trajectory-tracking operation) improves product quality and reduces batch-to-batch variability.

Temperature control of batch polymerization reactors is a challenging problem, because the process is nonlinear and exhibits time varying behavior owing to its batch nature. Also, it should be noted that heat transfer characteristic of the process will change due to changes of polymer viscosity over the course of the reaction. Conditions often change from batch to batch due to increased fouling of the reactor walls between cleaning periods, and because of changes in the environmental conditions such as heating and cooling fluid temperatures.

The temperature control of polymerization reactors has been studied extensively in the literature and has been reviewed in many papers such as Amrehn (1), Berber(2), Embirucu *et al.* (3) and Soroush (4). These studies can be divided into three main groups.

In the first group, results from differential geometry have been used successfully for nonlinear control synthesis. Briefly, the differential geometry based control deals with the idea of finding an inverse of a nonlinear process. Usually nonlinear transformations of the state and/or control variables are sought so that the transformed process description is linear (Isidori (5), Henson and Seborg (6, 7), Soroush and Kravaris (8), Palanki and Kravaris (9)). A few applications of nonlinear control of polymerization reactors based on differential geometry were reported in the literature; among them are Sorouh and Kravaris (10–12), Liu and Macchietto (13), Gentric *et al.* (14) and Pringle *et al.* (15).

In second group linear and nonlinear model predictive controllers (MPC), where model predictions over a given time horizon are used at each sampling time to generate optimal control policies over the control horizon, have been considered (Di Marco *et al.* (16), Henson (17)). Model predictive control offers a flexible and powerful solution to the dynamic optimization and control of polymerization reactors. A number of applications of MPC in the control of polymerization reactor have been reported (Hidalgo and Brosilow (18), Dittmar *et al.* (19), Gatta and Zafiriou (20), Peterson *et al.* (21) and Nagy *et al.* (22)).

The third group includes adaptive version of various control algorithms (Alonso *et al.* (23)). Adaptive controllers are always implemented with process parameter

*To whom correspondence should be addressed. E-mail: Shahrokhi@ Sina.Sharif.ac.ir. P. O. Box: 11365-9465, Azadi Ave. Tehran, I.R.Iran.

estimation routines in order to keep track of process conditions. Different types of adaptive control schemes were tested and compared in polymerization reactors (Tkamatsu *et al.* (24), Tzouanas and Shah (25), Wang and Lin (26)). Identification of the process parameters is the most important step in implementation of adaptive controllers.

In this paper, the performances of four different controllers, a fix PI, an adaptive PID based on pole-cancellation technique, and two nonlinear controllers based on GLC algorithm, one for known kinetic model (GLC-I) and the other for unknown kinetic model (GLC-II), are compared through simulation and real-time studies. A batch polymerization reactor in which suspension polymerization of MMA takes place is used for this investigation.

The article is organized as follows. First, the experimental system is described and then the mathematical model is given. Next, theory and structure of compared control algorithms are reviewed briefly. Finally, the process model validity is examined and the performances of the controllers are compared under different levels of parameter uncertainties.

EXPERIMENTAL SYSTEM

Figure 1 depicts a schematic diagram of the experimental set-up. The reactor is a 5L stainless steel jacketed vessel. The reactor contents are mixed by a three-paddle agitator at 600 rpm during the polymerization.

The heating/cooling system of the reactor consists of an electrical heater with power of about 6.0kW, a shell and tube heat exchanger, a motorized three-way control valve, a circulating pump and temperature sensors (four 0–100°C Resistance Temperature Detectors, RTD). The reactor temperature is measured by a RTD of the same type. The circulating pump maintains a constant jacket flow rate. The temperature of the heater is controlled by an ON/OFF controller at about 80°C.

The experimental system is connected to a computer by an I/O interface board (Axiom, Inc.; model AX5411).

MATHEMATICAL MODEL

For modeling, the free radical polymerization kinetic mechanism is used and for simplification the following standard assumptions are made (27).

- All the reactions are irreversible and elementary.
- The reaction rate constants are independent of chain length.
- The reactor contents are perfectly mixed, with no temperature gradients.
- The Long-Chain Hypothesis (LCH) is assumed.

Using the kinetic mechanism and performing mass and energy balances results the following set of ordinary differential equations:

$$\frac{dx_m}{dt} = (1 - x_m)(k_p + k_m)\lambda_0 \tag{1}$$

$$\frac{dx_i}{dt} = (1 - x_i)k_d \tag{2}$$

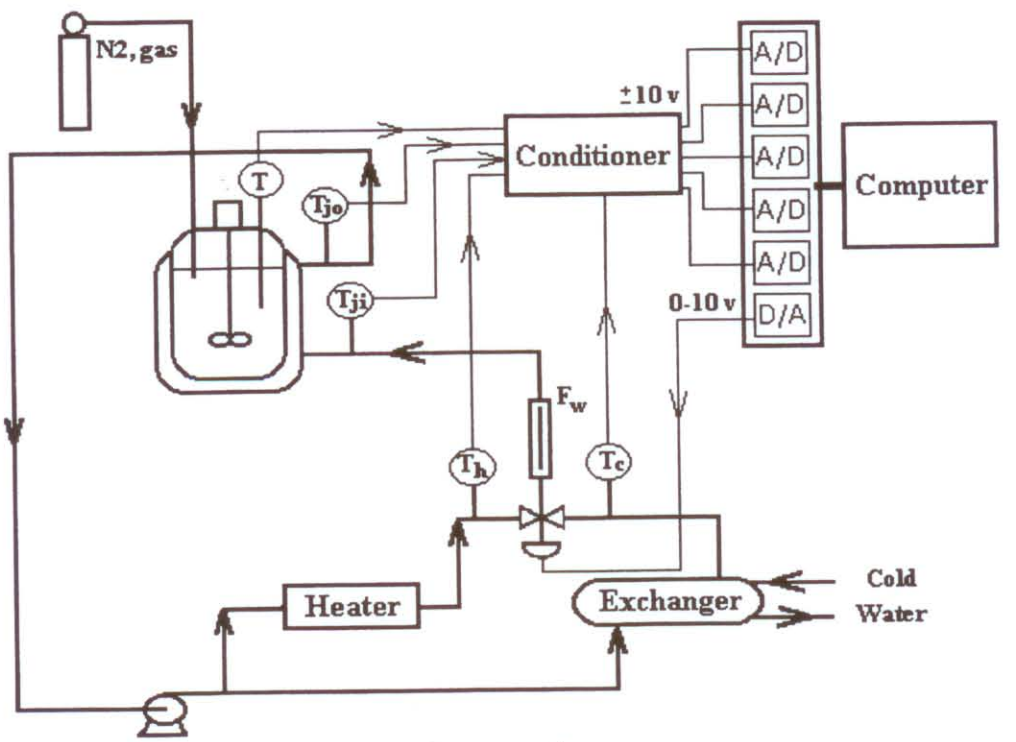

Fig. 1. Experimental system.

$$\frac{dT}{dt} = \frac{(-\Delta H_p)k_p\lambda_0 C_m V + UA(T_j - T)}{mc} \quad (3)$$

where

$$\lambda_0 = \left(\frac{2f k_d C_I}{k_t}\right)^{0.5} \quad (4)$$

$$C_m = \frac{(1 - x_m)C_{m0}V_0}{V} \quad (5)$$

$$C_I = \frac{(1 - x_I)C_{I0}V_0}{V} \quad (6)$$

$$V = V_0(1 + \varepsilon x_m) \quad (7)$$

In the above equations, x_m and x_I are monomer and initiator conversions, respectively. ε is the volume expansion factor and is given by:

$$\varepsilon = \phi_{m0}\left(\frac{\rho_m}{\rho_p} - 1\right) \quad (8)$$

In the MMA polymerization, termination and propagation reactions can become diffusion-controlled at increased viscosity of reaction medium. These phenomena are called gel and glass effects, respectively. To introduce the gel and glass effects in the model, the correlations proposed by Chiu *et al.* (28) are used. These correlations are given below:

$$k_t = \frac{k_{t0}}{1 + \frac{\lambda_0 k_{t0}}{D k_{\theta t}}} \quad (9)$$

$$k_p = \frac{k_{p0}}{1 + \frac{\lambda_0 k_{p0}}{D k_{\theta p}}} \quad (10)$$

where

$$D = \exp\left(\frac{2.3(1 - \phi_p)}{0.168 - 8.21 \times 10^{-6}(T - T_{gp})^2 + 0.03(1 - \phi_p)}\right) \quad (11)$$

The kinetic constants and other parameters of the mathematical model (for suspension polymerization of MMA with benzoyl peroxide initiator) are given in *Table 1* (10, 29, 30).

In the same way, performing energy balances for the jacket, heater and exchanger result the following equations:

$$\frac{dT_j}{dt} = \left[UA(T - T_j) + U_\infty A_\infty (T_\infty - T_j) + \frac{F_w \rho_w c_w}{1 - \gamma}(T_{ji} - T_j)\right] \Big/ m_j c_w \quad (12)$$

$$\frac{dT_c}{dt} = [U_c A_c (T_w - T_c) + (1 - a_v)F_w \rho_w c_w (T_{jo} - T_c)]/m_c c_w \quad (13)$$

Table 1. Kinetic and Other Parameters of MMA Polymerization.

$k_d = 1.69 \times 10^{14} \exp(-1.2561 \times 10^5 / RT)$, $W_m = 100.12$
$k_m = 4.661 \times 10^9 \exp(-7.4479 \times 10^4 / RT)$, $f = 0.5$
$k_{p0} = 4.9167 \times 10^5 \exp(-1.8283 \times 10^4 / RT)$, $c = 3.2$
$k_{t0} = 9.800 \times 10^7 \exp(-2.9442 \times 10^3 / RT)$, $m = 3.585$
$k_{\theta p} = 3.0233 \times 10^{13} \exp(-1.17 \times 10^5 / RT)$, $R = 8.345$
$k_{\theta t} = C_{i0} \times 1.454 \times 10^{20} \exp(-1.4584 \times 10^5 / RT)$
$\rho_m = 968 - 1.225\,(T - 273.2)$, $\rho_p = 1200$
$-\Delta H_p = 5.78 \times 10^4$, $T_{gp} = 387.2$, $UA = 0.097$

$$\frac{dT_h}{dt} = [Q_h + a_v F_w \rho_w c_w (T_{jo} - T_h)]/m_h c_w \quad (14)$$

where

$$T_{ji} = a_v T_h + (1 - a_v)T_c \quad (15)$$

$$T_{jo} = (T_j - \gamma T_{ji})/(1 - \gamma) \quad (16)$$

In the above equations T_j, T_c and T_h are temperatures of jacket, cold and hot streams, respectively. T_{ji} and T_{jo} are inlet and outlet jacket temperatures. T_{jo} is a function of T_{ji} and T_j. This functionality has been obtained through experimental data and is given by *Eq 16*. This equation is used in jacket energy balance (*Eq 12*).

If a_v is defined as the opening fraction of the three-way control valve (when the a_v is one, the hot stream way is fully open), then it can be related to the control signal (u_f) as given by the following equation:

$$a_v = \begin{cases} 0.089u_f^{1.078} & \text{if } u_f \le 7.6 \\ 0.519u_f - 3.152 & \text{if } u_f > 7.6 \end{cases} \quad (17)$$

Q_h in *Eq 14* is the variable power of heater and can be calculated by the following empirical equation:

$$Q_h = 6.45 + 0.7(T_h^* - T_h) + 0.007\int_0^t (T_h^* - T_h)dt \quad (18)$$

where T_h^* is the desired value of hot stream temperature (80°C).

The physical properties and other parameters of jacket energy balance equations (*Eqs 12–14*) are given in *Table 2*. The parameters given in *Table 2* are calculated through experimental data using the least square technique.

GLC METHOD

The GLC method is a nonlinear control algorithm based on differential geometric approach(10). The first step in the GLC synthesis is the calculation of a state feedback, under which the closed loop input/output system is exactly linear. Then for linearized system, a controller with integral action such as PI can be designed.

To implement the state feedback of the GLC, all the process state variables should be measured or estimated on-line. State estimation technique such as

Table 2. Physical Properties and Other Parameters of Heating/Cooling System.

$UA = 0.097$,	$U_\infty A_\infty = 0.02$,	$U_c A_c = 0.165$
$m_j = 1.7$,	$m_c = 6.5$,	$m_h = 5.5$
$c_w = 4.2$,	$F_w = 2.33 \times 10^{-4}$,	$\gamma = 0.75$
$T_\infty = 293.7$,	$T_w = 294.2$,	$\rho_w = 983$

extended Kalman filter (EKF) can be used for estimation of unmeasured state variables (4, 31).

Consider SISO processes with the following model:

$$\begin{cases} \dfrac{dx}{dt} = f(x) + g(x)u \\ y = h(x) \end{cases} \tag{19}$$

with a finite relative order r (the relative order is the smallest integer for which $L_g L_f^{r-1} h(x) \neq 0$). Here x is the vector of state variables, u and y are the manipulated input and the controlled output, respectively. Under the state feedback:

$$u = \frac{v - h(x) - \sum_{i=1}^{r} \beta_i L_f^i h(x)}{\beta_r L_g L_f^{r-1} h(x)} \tag{20}$$

where β_i's are tunable parameters, the closed-loop v–y behavior is linear and described by the following equation:

$$v = y + \sum_{i=1}^{r} \beta_i \frac{d^i y}{dt^i} \tag{21}$$

Some guidelines for tuning of β_i's parameters and other remarks for using GLC technique are described by Soroush and Kravaris (8).

In what follows the structures of globally linearized controllers used for experimental system are described.

DESIGNING GLC ALGORITHMS FOR EXPERIMENTAL SYSTEM

The control objective is to track the desired temperature profile (T^*) by manipulating the jacket inlet temperature that is achieved by changing a_v.

First the differential equations of process model (*Eqs 1–3*) are described in standard state space form as given below:

$$\begin{cases} \dfrac{d}{dt}\begin{bmatrix} x_m \\ x_i \\ T \end{bmatrix} = \begin{bmatrix} f_1(x_m, x_i, T) \\ f_2(x_i, T) \\ f_3(x_m, x_i, T, T_\infty, T_c) \end{bmatrix} + \begin{bmatrix} 0 \\ 0 \\ g_3(T_h, T_c) \end{bmatrix} a_v \\ y = T \end{cases} \tag{22}$$

where

$$f_1 = (1 - x_m) k_p \lambda_0 \tag{23}$$

$$f_2 = (1 - x_i) k_d \tag{24}$$

$$f_3 = \alpha_0 f_1 + \alpha_1 T + \alpha_2 T_\infty + \alpha_3 T_c \tag{25}$$

$$g_3 = \alpha_3 (T_h - T_c) \tag{26}$$

$$\alpha_0 = \frac{(-\Delta H_p) C_{m0} V_0}{mc} \tag{27}$$

$$\alpha_1 = \frac{UA}{mc}\left(\frac{UA}{\alpha} - 1\right) \tag{28}$$

$$\alpha_2 = \frac{UA}{mc}\left(\frac{U_\infty A_\infty}{\alpha}\right) \tag{29}$$

$$\alpha_3 = \frac{UA}{mc}\left(\frac{F_w \rho_w c_w}{\alpha(1 - \gamma)}\right) \tag{30}$$

$$\alpha = UA + U_\infty A_\infty + \frac{F_w \rho_w c_w}{1 - \gamma} \tag{31}$$

It is important to mentioned that the time constants of reactor and jacket dynamics are about 150 and 5 sec, respectively. Therefore, in *Eq 22* the QSSA is used for calculation of jacket temperature.

The model described by *Eq 22* has the relative order of one, therefore, the input/output linearizing state feedback has the following form:

$$a_v = \frac{v - T - \beta f_3}{\beta \alpha_3 (T_h - T_c)} \tag{32}$$

A PI controller can be used to generate the input of linearized system (v) as given below:

$$v = v_s + K_c(T^* - T) + \frac{K_c}{\tau_I} \int_0^t (T^* - T) dt \tag{33}$$

In the simulation and experimental runs, $v_s = T^*$ was assumed.

In the state feedback law (*Eq 32*), a_v is a function of state variables (x_m, x_i, T) and disturbances (T_∞, T_c, T_h). T, T_c and T_h are measured on-line and T_∞ is assumed to be constant. The remaining variables (x_m, x_i) must be estimated by an estimation technique. In this paper an EKF is used for estimation of unmeasured variables. The structure of estimator is described by Shahrokhi and Fanaei (32). The block diagram of reactor temperature control by GLC method is shown in *Fig. 2*. This control scheme is called GLC-I.

To develop the second form of GLC, called GLC-II, we assume that the kinetic model is not available. The rate of heat released by reaction, Q_r, can be added to energy equation by a random walk model as given below:

$$\begin{cases} \dfrac{d}{dt}\begin{bmatrix} Q_r \\ T \end{bmatrix} = \begin{bmatrix} 0 \\ f_3'(Q_r, T, T_\infty, T_c) \end{bmatrix} + \begin{bmatrix} 0 \\ g_3(T_h, T_c) \end{bmatrix} a_v \\ y = T \end{cases} \tag{34}$$

where

$$f_3' = \frac{Q_r}{mc} + \alpha_1 T + \alpha_2 T_\infty + \alpha_3 T_c \tag{35}$$

g_3 and other parameters in *Eq 35* are the same as those in *Eqs 26–31*.

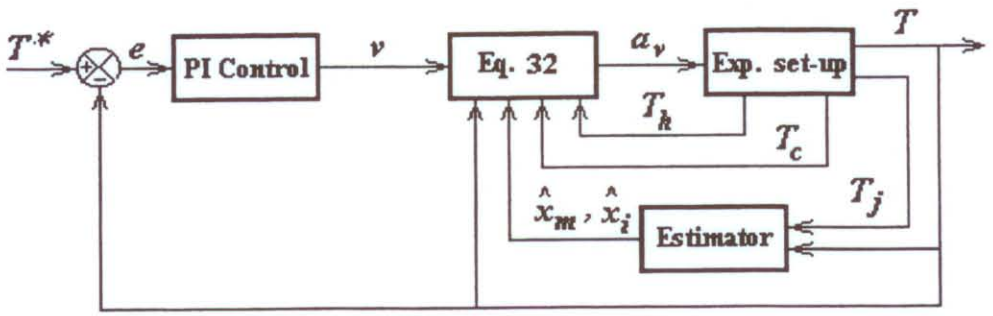

Fig. 2. Block diagram of implemented GLC.

Similarly, the linearizing state feedback of GLC-II has the following form:

$$a_v = \frac{v - T - \beta f_3'}{\beta\alpha_3(T_h - T_c)} \quad (36)$$

As before, an EKF is used for estimation of Q_r. It is important to mentioned that in the GLC-II, no reaction kinetic model is required.

ADAPTIVE PID

PID controllers have been used for many years in industry, and if the controller is well tuned, its performance is acceptable for many industrial processes. When the operating point is changed, because of nonlinear behavior of most processes, the controller should be retuned. In this regard, several self-tuning PID controllers are proposed in the literature. Shahrokhi and Fanaei (33) compared four adaptive PID controllers and showed that the best performance belongs to pole cancellation technique. This technique is used in this article.

For pole cancellation method, the process is modeled by the following equation:

$$y(t) = \frac{q^{-d}(b_0 + b_1q^{-1} + \ldots + b_mq^{-m})}{1 + a_1q^{-1} + a_2q^{-2}}u(t) + v(t) \quad (37)$$

where y and v are plant output and unmeasured disturbance, respectively. PID controller has the following discrete model:

$$u(t) = u(t-1) + (g_0 + g_1q^{-1} + g_2q^{-2})e(t) \quad (38)$$

In this method the controller parameters (g_0 ,g_1 ,g_2) are so designed to cancel the process model poles and achieve the desired phase margin (ϕ_m). In adaptive version, the process model parameters are estimated by recursive least squares (RLS) at each sampling time and based on these estimates the PID parameters are updated (34, 35). The schematic block diagram of the adaptive PID is shown in *Fig. 3*.

EXPERIMENTAL PROCEDURE

To verify the model, the experimental system of *Fig. 1* is used for suspension polymerization of MMA with benzoyl peroxide initiator. The MMA contains hydroquinone monomethyl ether inhibitor to prevent polymerization during storage. To remove the inhibitor, the monomer was washed once with NaOH (5% solution) and twice with distilled water. Furthermore, the remained water in the monomer was removed with anhydrous sodium sulfate. The loading amounts of monomer, initiator and distilled water in each batch are 1.4, 0.018 and 2.0 kg respectively. The quantities of TSP, calcium chloride and SDBS (used for producing suspending medium), are 0.0191, 0.1315 and 0.0168 kg, respectively. These quantities are found by trial and error for obtaining small size pellets of polymer(50–200 μm), at agitation rate of 600 rpm.

The procedure used in each batch has the following steps:

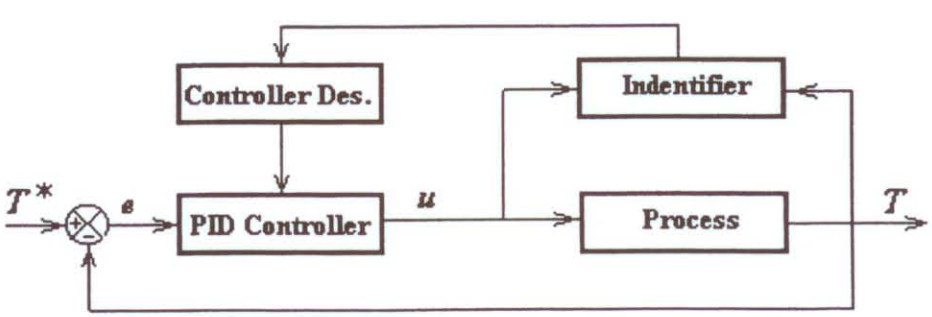

Fig. 3. Block diagram of adaptive PID.

1. Prepare materials using the loading conditions.
2. Dissolve the TSP in the distilled water and load it into the reactor vessel.
3. Load the monomer into a vessel and stir it by an agitator. Introduce nitrogen gas into the monomer for one hr to purge any dissolved oxygen.
4. Preheat the reactor to the desired temperature and load the calcium chloride.
5. Load the SDBS into the reactor vessel after about 10 min.
6. Remove about 150 cc of the monomer and load it into a 250 cc beaker and heat the remained monomer in the vessel to the desired temperature.
7. Dissolve the initiator in the beaker containing monomer.
8. Load the solution prepared in step 7 into the monomer vessel and mix properly. Then load the mixture into the reactor vessel and initiate the control algorithm.
9. Blank the reacting medium with the nitrogen gas to keep oxygen out of the reactor.

During the polymerization, samples were taken and conversion is determined by a gravimetric method.

Model Validation

To verify the model describing suspension polymerization of MMA, several experiments have been performed. For example, experimental data of the monomer conversion and reactor temperature are compared with the model predictions in *Figs. 4* and *5*, respectively. These data are obtained by using a PI controller with the same tuning (K_c = 1.0,τ_I = 150) in simulation and experimental runs. The temperature set point for time less than 30 min and greater than 60 min is 70°C and for time between 30 and 60 min is 60°C. As can be seen from the results, the model successfully predicts the monomer conversion and reactor temperature except close to gel effect region.

RESULTS

In this section the performances of the selected controllers (GLC-I, GLC-II, adaptive PID and fix PI) are compared through simulation and real-time studies under different levels of parameter uncertainties. In all runs, for estimation of unknown state variables needed in GLC schemes, an standard EKF with added fictitious noise (31, 36) is used. The unknown model parameters in adaptive PID are estimated using a standard RLS with variable forgetting factor (34). The sample time for GLC schemes and fix PI is 5 second and for adaptive PID is 20 second.

Simulation Results

In each simulation two set-point changes with magnitude of –5 and +5°C are applied at 25 and 50 min, respectively. The values of tuning parameters that are used in simulation for GLC schemes and fix PI are given in *Table 3*. For adaptive PID the desired phase margin is 65. The degree of numerator polynomial is three and the process dead time is set to one sampling time. In implementation of adaptive PID, for better convergence of estimated parameters, a PRBS with

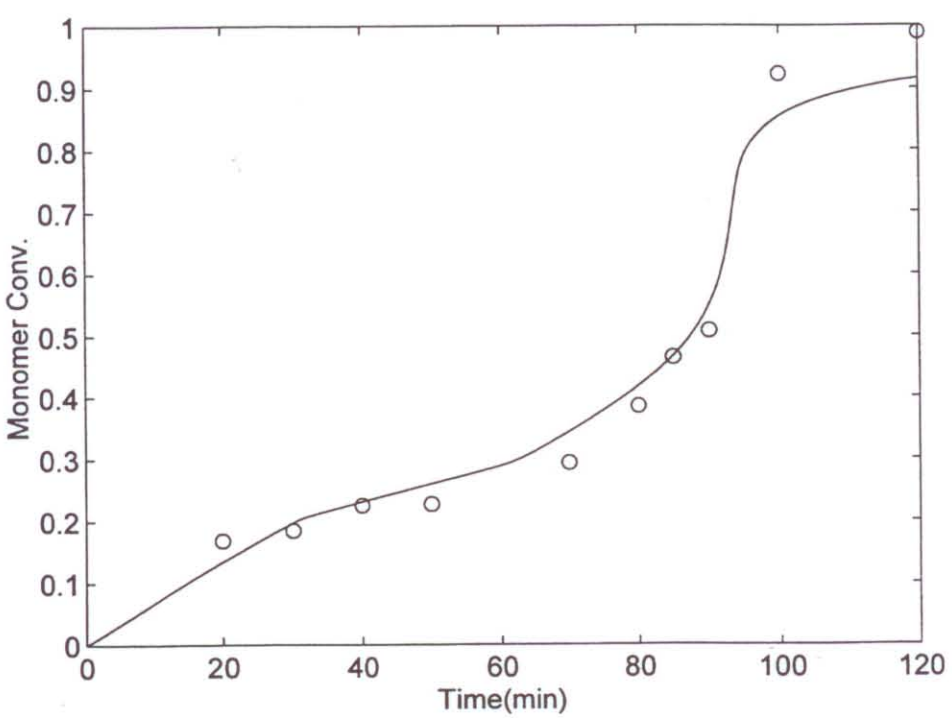

Fig. 4. Experimental data and model predictions (solid line) of monomer conversion.

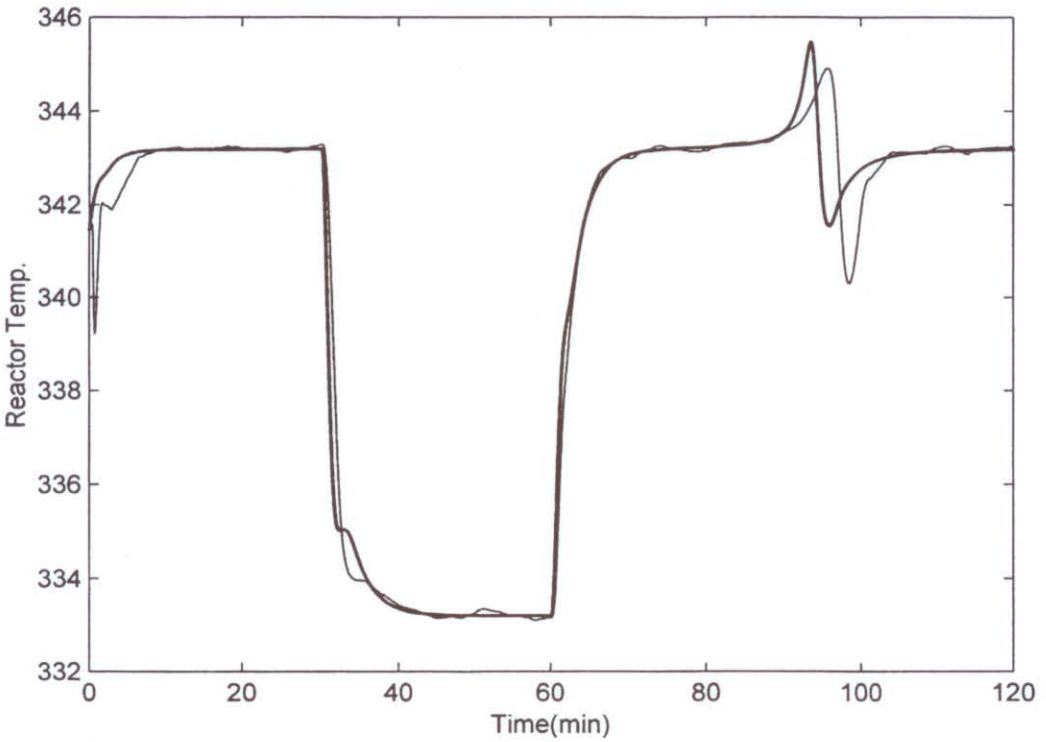

Fig. 5. Experimental data (thin line) and model predictions (solid line) of reactor temperature.

magnitude of 0.5 is applied for the first 15 min. For comparison of the controllers' performances, the value of IAE is calculated for time period 25–70 min for set-point changes (IAE_1) and for time period 70–110 min for gel effect (IAE_2).

The values of IAE for nominal case, ± 40% error in heat transfer coefficient (U), ± 20% error in initial mass of monomer (w_{m0}) and ± 20% error in initial mass of initiator (w_{i0}) are given in *Table 4*. As can be seen from the results, the GLC-I and GLC-II have better performances than fix and adaptive PID, especially for gel effect region. In addition, the GLC-II has simpler structure compared with GLC-I and no kinetic model is required. The worst performance belongs to adaptive PID especially in gel effect region.

Experimental Results

In each run, two set-point changes with magnitude of −10 and +10°C are applied at 30 and 60 min, respectively. The values of tuning parameters that are used in experimental runs for GLC schemes and fix PI are given in *Table 5*. For adaptive PID the desired phase margin is 70. The degree of numerator polynomial is three and the process dead time is set to one sampling time. In implementation of adaptive PID a PRBS with magnitude of 1.0 volt is applied for first 20 min.

Table 3. Tuning Parameters of GLC-I, GLC-II and Fix PI for Simulation.

Controller	K_c	τ_I	β
GLC-I	2.0	150	150
GLC-II	2.0	150	150
fix PI	1.0	150	—

The experimental results are shown in *Figs. 6–9*. As can be seen, the experimental results confirm the simulation results.

In the polymerization reactors the heat transfer coefficient uncertainty is common. Therefore, the performances of controllers should be compared considering this uncertainty. The control results for GLC-I and GLC-II with +30% error in heat transfer coefficient are shown in *Figs. 10* and *11*. As can be seen from the results, performances of GLC-I and GLC-II are almost the same.

Note: It is important to mention that in the implementation of GLC-I a closed loop estimator (such as EKF) must be used for estimating the unknown states. A poor performance may be obtained in gel effect region (due to model uncertainty), if an open loop observer is used. If open loop observer is used for GLC-I under the same condition of *Fig. 6*, the result will be as shown in *Fig. 12*. As can be seen the performance of GLC-I with open loop observer is deteriorated in the gel effect region. This is due to model uncertainty in prediction of gel effect.

CONCLUSIONS

In this paper, performances of two GLC schemes, a fix PI and an adaptive PID are compared through simulations and real-time studies. Results indicate that

Table 4. The Values of IAE for Simulation Reaults.

Uncertainty	IAE	GLC-I	GLC-II	Fix PI	Adap.PID
nominal	IAE_1	808	807	1005	1011
nominal	IAE_2	244	377	837	1428
–40% in U	IAE_1	1295	1145	1180	1518
–40% in U	IAE_2	656	749	1216	2119
+40% in U	IAE_1	776	818	998	1003
+40% in U	IAE_2	322	261	627	1034
–20% in w_{m0}	IAE_1	783	804	1007	1016
–20% in w_{m0}	IAE_2	500	297	670	1100
+20% in w_{m0}	IAE_1	863	826	1011	1026
+20% in w_{m0}	IAE_2	165	458	982	1814
–20% in w_{i0}	IAE_1	809	808	1010	1006
–20% in w_{i0}	IAE_2	256	374	836	1437
+20% in w_{i0}	IAE_1	811	806	1005	1026
+20% in w_{i0}	IAE_2	234	376	828	1385

Table 5. Tuning Parameters of GLC-I, GLC-II and Fix PI for Experimental Runs.

Controller	K_c	τ_I	β
GLC-I	1.5	150	150
GLC-II	1.5	150	150
fix PI	1.0	150	—

GLC-I and GLC-II have better performances than fix PI and adaptive PID. In addition, GLC-II has a simpler structure than GLC-I and can be used without requiring the kinetic model. In implementation of GLC-I the closed loop observer should be used due to model uncertainties. The worst performance belongs to adaptive PID, owing to rapid model changes in gel effect region.

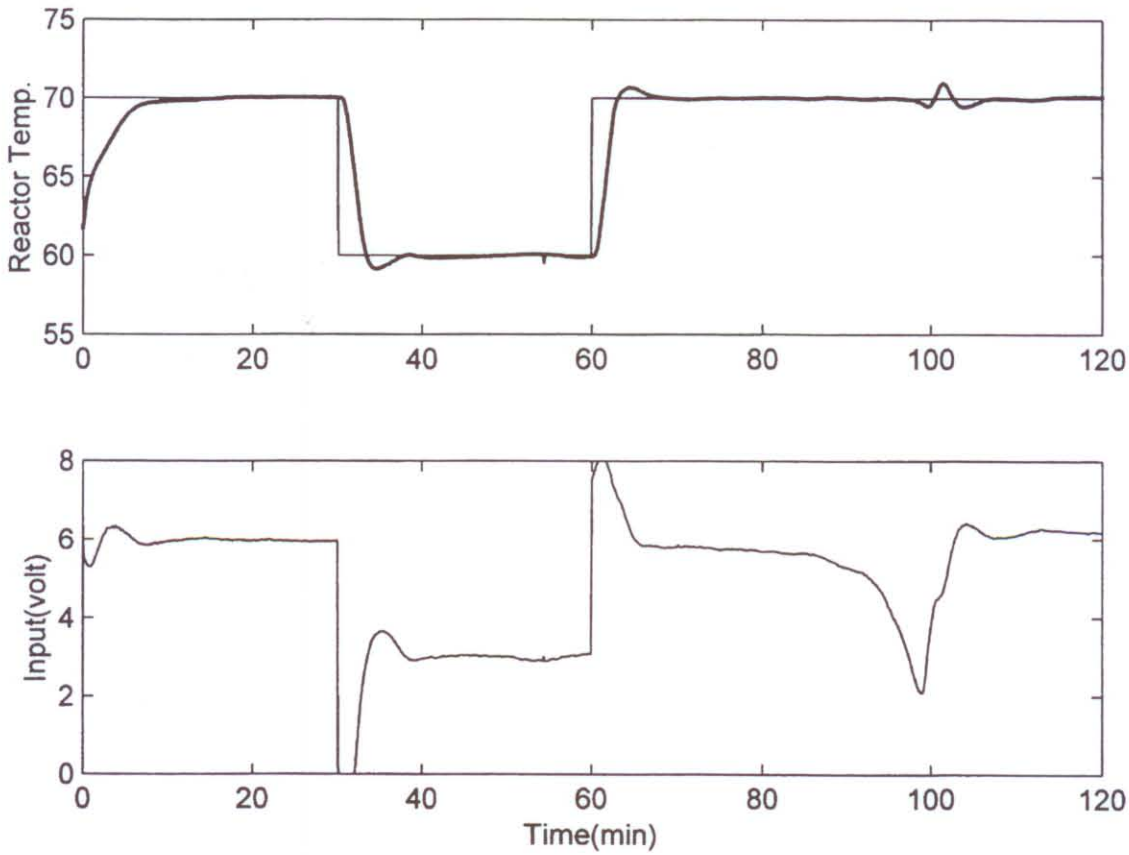

Fig. 6. Experimental temperature control results of GLC-I.

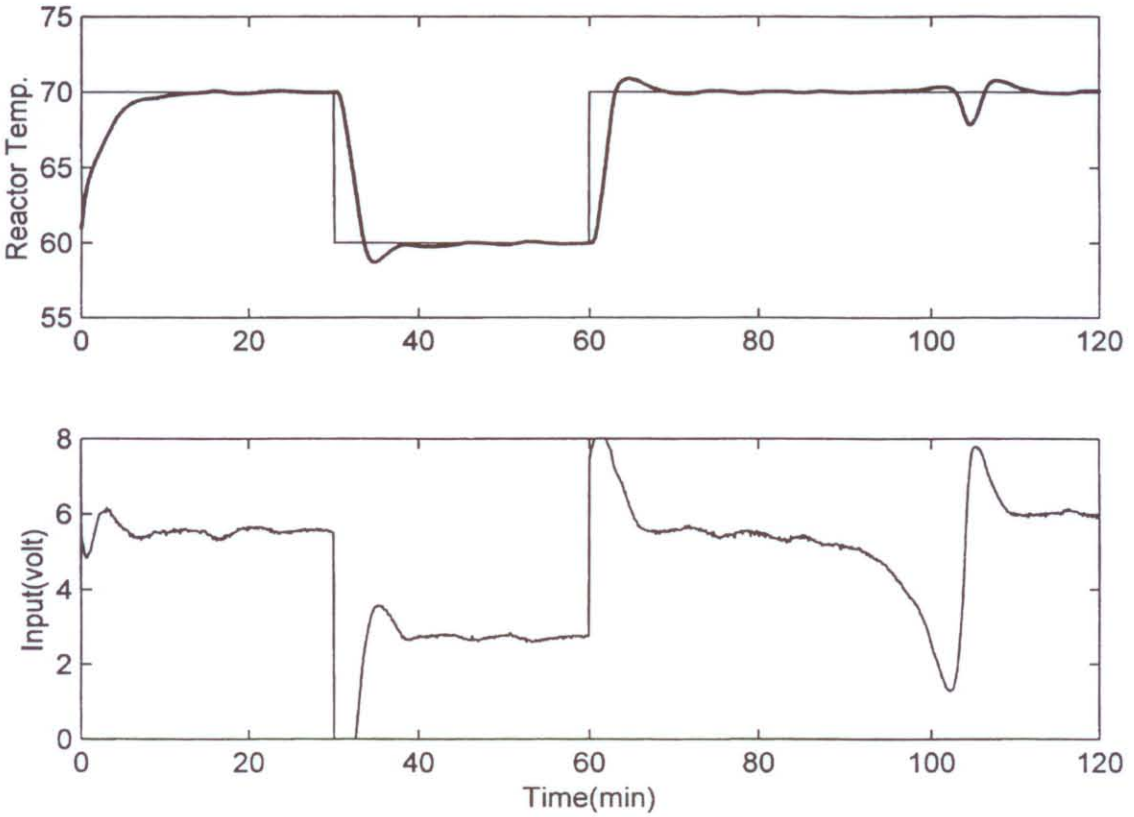

Fig. 7. Experimental temperature control results of GLC-II.

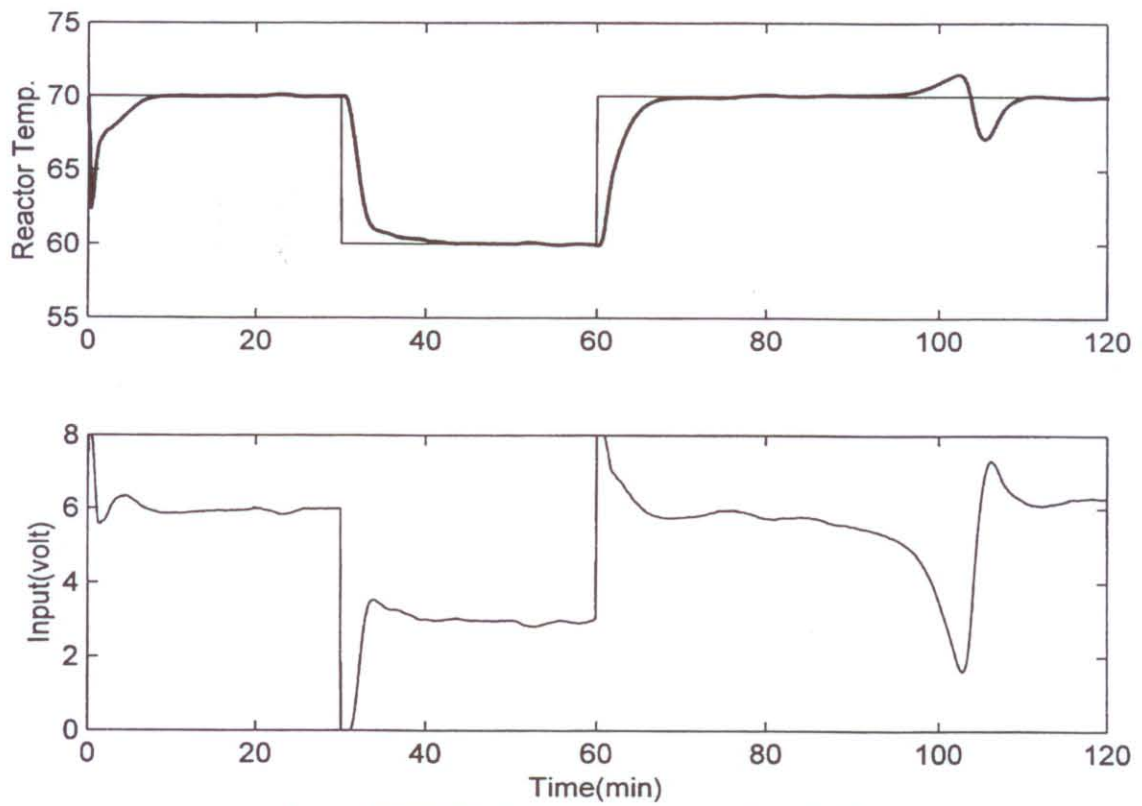

Fig. 8. Experimental temperature control results of fix PI.

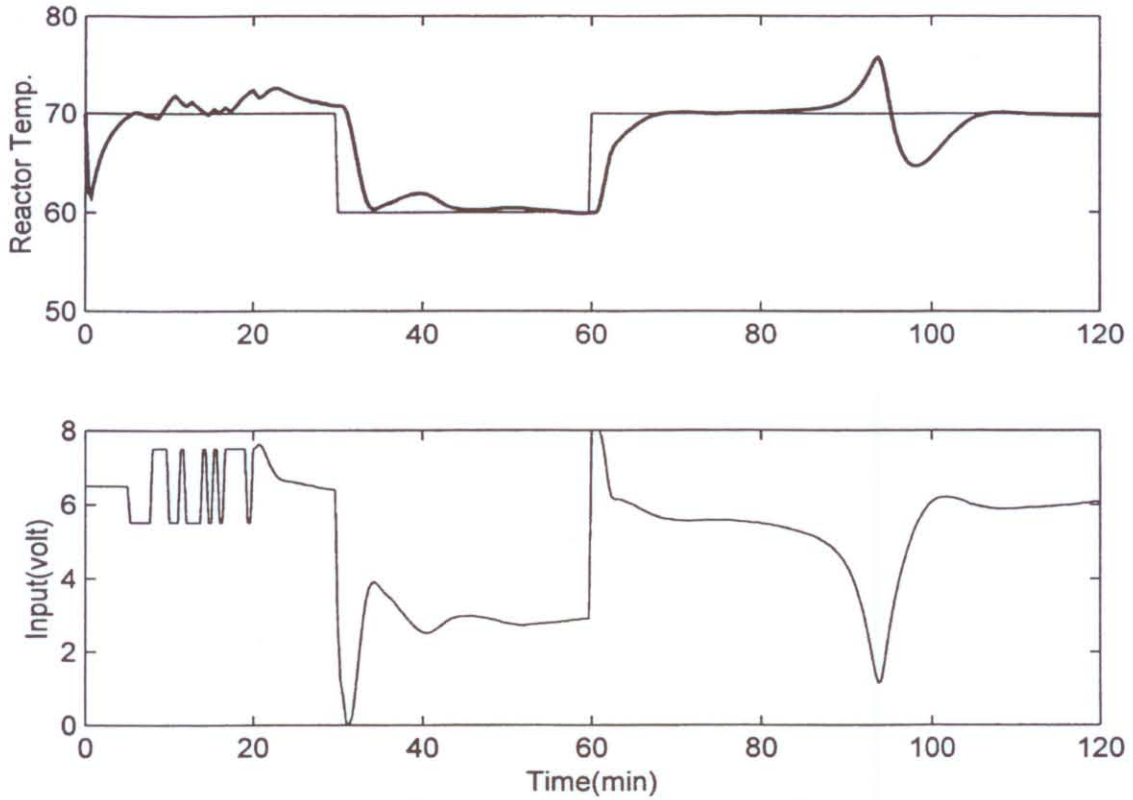

Fig. 9. Experimental temperature control results of adaptive PID.

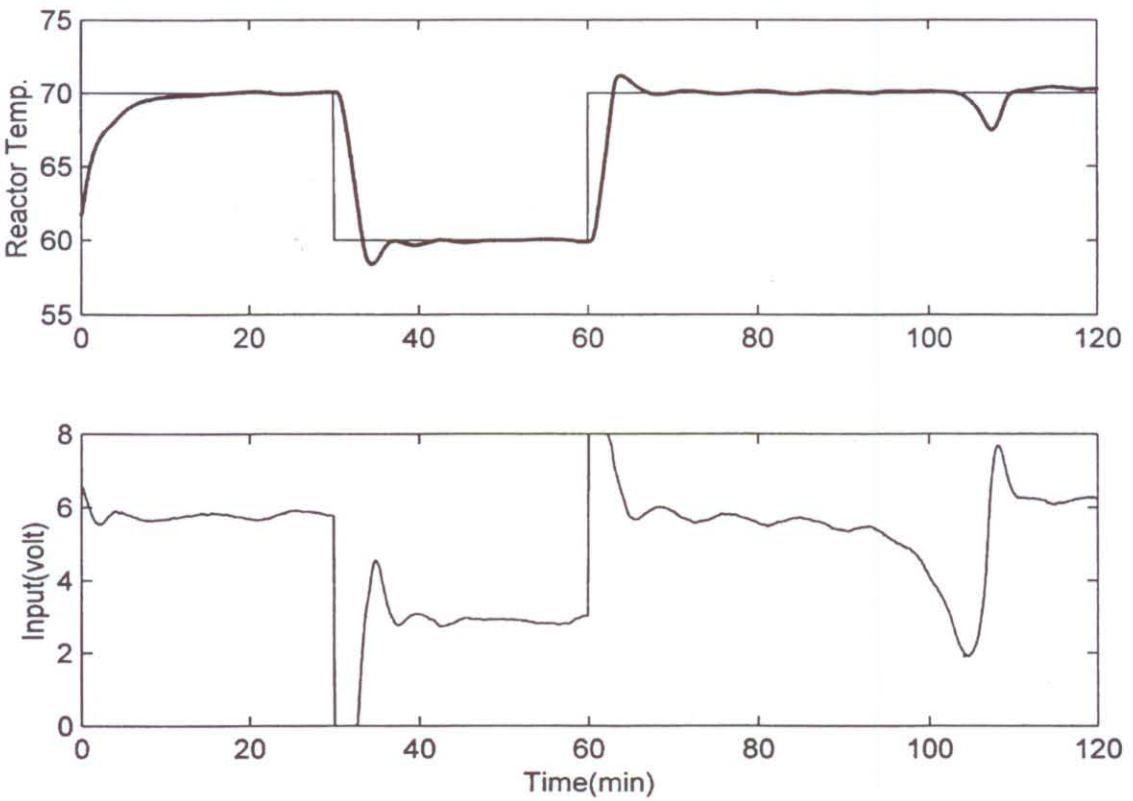

Fig. 10. Experimental control results of GLC-I with +30% error in U.

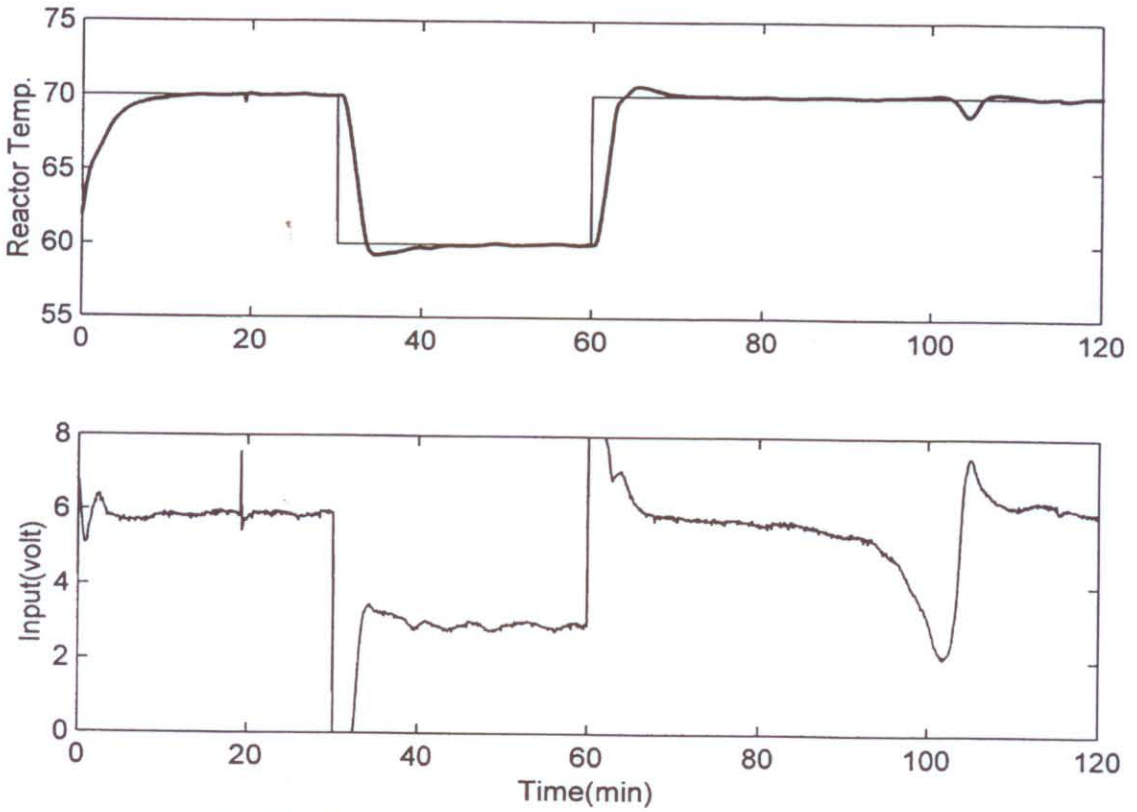

Fig. 11. Experimental control results of GLC-II with +30% error in U.

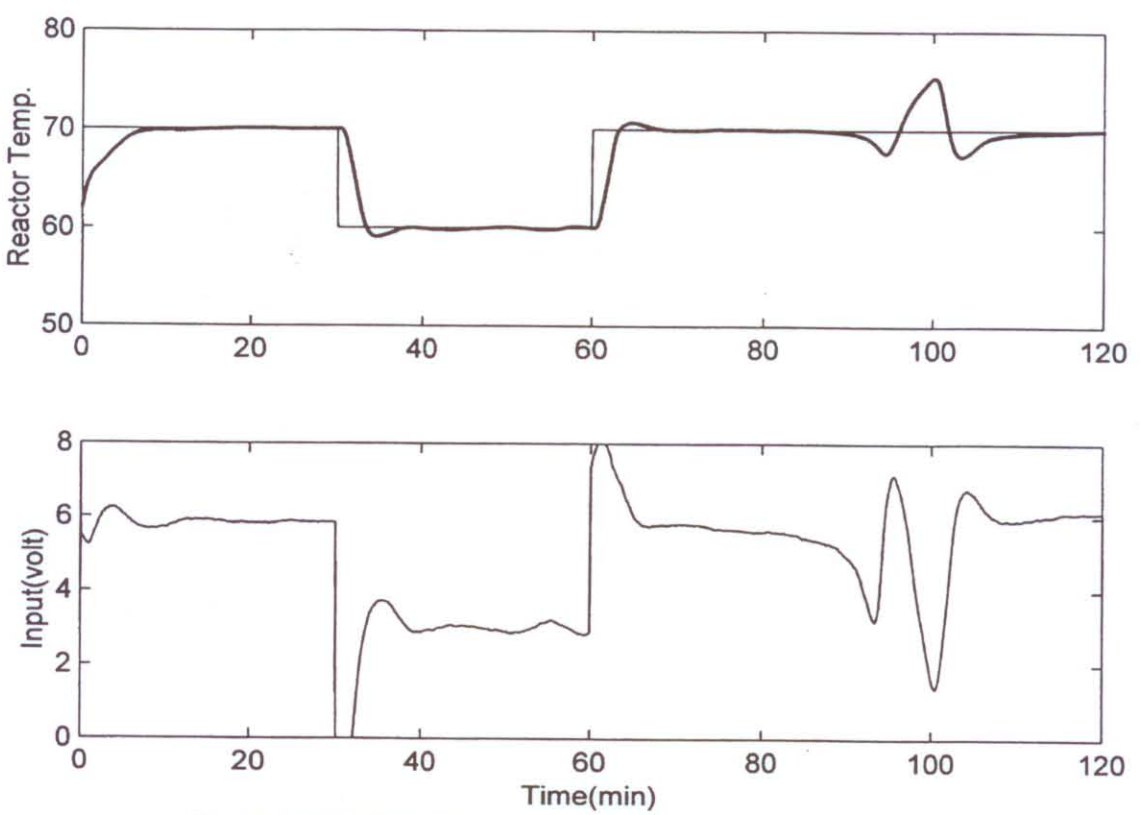

Fig. 12. Experimental control results of GLC-I using an open loop observer.

ACKNOWLEDGMENT

The support of the Iran Polymer Institute in providing experimental set-up is gratefully acknowledged. The authors wish to thank F. Hormozi and M. Parvazinia for their invaluable assistance in the experimental runs.

NOMENCLATURE

A, A_∞ = reactor-jacket and surrounding-jacket heat transfer area, m^2
A_c = heat transfer area of heat exchanger, m^2
a_v = hot stream opening fraction (1= fully opened, 0= fully closed)
a_i, b_i = discrete process model parameters
C_i, C_{i0} = concentration of initiator and its initial value, $kmol \cdot m^{-3}$
C_m, C_{m0} = concentration of monomer and its initial value, $kmol \cdot m^{-3}$
c = heat capacity of reactor contents, $kJ \cdot kg^{-1} \cdot K^{-1}$
c_w = heat capacity of water, $kJ \cdot kg^{-1} \cdot K^{-1}$
D = intermediate variable in gel and glass effect models
d = no of time delay of discrete model
e = controller input
F_w = flow rate of jacket, $m_3 \cdot s^{-1}$
f = initiator efficiency
$f(.)$ = vector of modeling equations
$g_0 - g_2$ = discrete controller parameters
K_c = gain of PID controller
k_d = rate constant for initiation reaction, s^{-1}
k_m = rate constant for chain transfer to monomer, $m^3 \cdot kmol^{-1} \cdot s^{-1}$
k_p = rate constant for propagation reaction, $m^3 \cdot kmol^{-1} \cdot s^{-1}$
k_{tc} = rate constant for termination by combination, $m^3 \cdot kmol^{-1} \cdot s^{-1}$
k_{td} = rate constant for termination by disproportion, $m^3 \cdot kmol^{-1} \cdot s^{-1}$
$k_t = k_{td} + k_{tc}$
k_{p0}, k_{t0} = true propagation and termination rate constant, $m^3 \cdot kmol^{-1} \cdot s^{-1}$
$k_{\theta p}, k_{\theta t}$ = parameters of gel and glass effect model
$L_f h(x)$ = Lie derivative of scalar field (h) with respect to vector field (f)
m = mass of reactor contents, kg
m = degree of numerator polynomial of discrete process model
m_c = mass of cold water stream, kg
m_j = mass of water in jacket, kg
m_h = mass of hot water stream, kg
Q_h = power of heater, kW
Q_r = rate of heat released by reaction, kW
q^{-1} = backward shift operator
r = relative order of controlled output with respect to manipulated input
T, T^* = reactor temperature and its desired value, K
T_c = cold stream temperature, K
T_{gp} = glass transition temperature of PMMA, K
T_h, T_h^* = hot stream temperature and its desired value, K
T_∞ = surrounding temperature, K
T_j = jacket temperature, K
T_{ji}, T_{jo} = inlet and outlet temperatures of jacket, K
T_w = temperature of cooling water, K
t, t_s = time and sampling time respectively, s
U, U_∞ = overall heat transfer coefficient of reactor-jacket and surrounding-jacket , $kJ \cdot m^{-2} \cdot s^{-1} \cdot K^{-1}$ respectively,
U_c = overall heat transfer coefficient of exchanger, $kW \cdot m^{-2} \cdot K^{-1}$
u = manipulated variable
u_f = input analog signal to three way control valve (0–8 volt)
V, V_0 = volume of the reacting mixture and its initial value, m^3
v = external input of linearized closed-loop system
w_{i0}, w_{m0} = loading mass of initiator and monomer respectively, kg
x = vector of state variables
x_i, x_m = initiator and monomer conversions, respectively
y = controlled variable

Greek Letters

α_i = process parameters
β = tunable parameter of input/output linearized system
γ = tunable parameter in calculation of jacket outlet temperature
$-\Delta H_p$ = heat of propagation reactions, $kJ \cdot kmol^{-1}$
ε = polymerization volume expansion
ϕ_m = desired phase margin
ϕ_{m0} = initial value of monomer volume fraction
ϕ_p = volume fraction of polymer
ρ_m, ρ_p = density of monomer and polymer respectively, $kg \cdot m^{-3}$
ρ_w = destiny of water, $kg \cdot m^{-3}$
ν = bounded unmeasured disturbances
t_I = integral time constant of PID controllers, s

REFERENCES

1. H. Amrehn, *Automatica*, **13**, 533 (1977).
2. R. Berber, *Trans. IChemE*, **74**, 3 (1996).
3. M. Embirucu, E. L. Lima, and J. C. Pinto, *Polym. Eng. Sci.*, **36**, 433 (1996).
4. M. Soroush, *Comp. Chem. Eng.*, **23**, 229 (1998).
5. A. Isidori, *Nonlinear Control Systems*, 2nd edition, Springer-Verlag (1989).
6. M. A. Henson and D. E. Seborg, *AIChE J.*, **36**, 1753 (1990).
7. M. A. Henson and D. E. Seborg, *AIChE J.*, **37**, 1065 (1991).
8. M. Soroush and C. Kravaris, *AIChE J.*, **38**, 1923 (1992).
9. S. Palanki and C. Kravaris, *Comp. Chem. Eng.*, **21**, 891 (1997).
10. M. Soroush and C. Kravaris, *AIChE J.*, **38**, 1429 (1992).
11. M. Soroush and C. Kravaris, *AIChE J.*, **39**, 1920 (1993).
12. M. Soroush and C. Kravaris, *AIChE J.*, **40**, 980 (1994).
13. Z. H. and S. Macchietto, *Comp. Chem. Eng.*, **19**, Suppl., S477 (1995).

14. C. Gentric, F. Pla, and J. P. Corriou, *Comp. Chem. Eng.*, **21**, Suppl., S1043 (1997).
15. T. Clarke-Pringle and J. F. MacGregor, *Comp. Chem. Eng.*, **21**, 1395 (1997).
16. R. Di Marco, D. Semino, and A. Brambilla, *Ind. Eng. Chem. Res.*, **36**, 1708 (1997).
17. M. A. Henson, *Comp. Chem. Eng.*, **23**, 187 (1998).
18. P. M. Hidalgo and C. B. Brosilow, *Comp. Chem. Eng.*, **14**, 481 (1990).
19. R. Dittmar, Z. Ogonowski, and K. Damert, *Chem. Eng. Sci.*, **46**, 2679 (1991).
20. G. Gatta and E. Zafiriou, *Ind. Eng. Chem. Res.*, **31**, 1096 (1992).
21. T. Peterson, E. Hernondez, Z. Arkun, and F. J. Schork, *Chem. Eng. Sci.*, **47**, 737 (1992).
22. Z. Nagy and S. Agachi, *Comp. Chem. Eng.*, **21**, 571 (1997).
23. A. A. Alonso, J. R. Banga, and R. Perez-Martin, *Comp. Chem. Eng.*, **22**, 445 (1998).
24. T. Takamatsu, S. Shioya, and Y. Okada, *Ind. Eng. Chem. Res.*, **27**, 93 (1988).
25. V. K. Tzouanas and S. L. Shah, *Chem. Eng. Sci.*, **44**, 1183 (1989).
26. F. S. Wang and Y. C. Lin, *Chem. Eng. Technol.*, **14**, 240 (1991).
27. N. A. Dotson, R. Galvan, R. L. Laurence, and M. Tirrell, *Polymerization Process Modeling*, VCH Publishers (1996).
28. W. R. Chiu, G. M. Carratt, and D. S. Soong, *Macromol.*, **16**(3), 348 (1983).
29. A. D. Schmidt and W. H. Ray, *Chem. Eng. Sci.*, **36**, 1401 (1981).
30. P. E. Baillagou and D. S. Soong, *Chem. Eng. Sci.*, **40**, 87 (1985).
31. A. Gelb, *Applied Optimal Estimation*, MIT Press, Cambridge, Massachusetts (1974).
32. M. Shahrokhi and M. A. Fanaei, *Iranian Polymer J.*, **10**, 3 (2001).
33. M. Shahrokhi and M. A. Fanaei, *Scientia Iranica*, **7**, 1 (2000).
34. T. R. Fortescue, L. S. Kershenbaum, and B. E. Ydstie, *Automatica*, **17**, 831 (1981).
35. C. S. Bayacz, J. Hetthessy, and L. Keviczky, *IFAC Symp. Ident. Syst. Parameter Est.*, York, 1299 (1985).
36. D. J. Kozub and J. F. MacGregor, *Chem. Eng. Sci.*, **47**, 1047 (1992).